

Wavelet Image of a Heliospheric Storm in Cosmic Rays

V. I. Kozlov and V. V. Markov

*Institute of Cosmophysical Research and Aeronomy, Siberian Division, Russian Academy of Sciences,
pr. Lenina 31, Yakutsk, 677007 Russia*

Received September 29, 2005; in final form, February 17, 2006

Abstract—During the sign reversal of the global solar magnetic field, the variations in the ratio of the quadrupole component of the field to its dipole part manifest themselves in a change of the two-sector structure of the heliospheric current sheet (HCS) into the four-sector and, then, multisector structures. At that time, a soliton-like wave packet (soliton of the envelope), precisely which is responsible for a wavelet image of heliospheric storm in cosmic rays, is formed in HCS.

PACS numbers: 96.50.Xy; 94.20.Wq

DOI: 10.1134/S0016793207010082

1. INTRODUCTION

The known variations in the ratio of the quadrupole component of the field to its dipole part are obviously related to the transient process of field sign reversal. The variations in the ratio of the quadrupole component of the field to the dipole one manifest themselves in the HCS structure: two-sector for the dipole component and four-sector for the quadrupole one [Sunderson et al., 2003].

It was expected that, during the sign reversal of the global solar magnetic field, the variations in the quadrupole-to-dipole ratio should manifest themselves in a change in the HCS structure from two-sector to four-sector and, then, to multisector. Preliminary results showed that the GCR scintillation index, which by definition reflects the fine structure of GCR intensity, turned out to be a flexible tool for analyzing the dynamics of the HCS structure, an important GCR modulating parameter.

2. FLUCTUATION ANALYSIS METHOD

The drawbacks of the spectral–temporal analysis of dynamic processes invoking the Fourier transform are well known and are associated with a peculiar “principle of uncertainty” of the conventional spectral–temporal analysis: an increase in frequency resolution inevitably results in an increase in the uncertainty of the time resolution and vice versa. The best results are achieved using a wavelet analysis.

Figure 1 presents the results of a wavelet analysis of the GCR intensity fluctuations for two Bartels solar rotations (2323–2324) during the well-known events in October–November 2003. The top graph shows the GCR intensity averaged over 12 h. Then, using the Gaussian (optimal) high-frequency filter, we eliminated the LF trend from the initial 5-min data. The results of

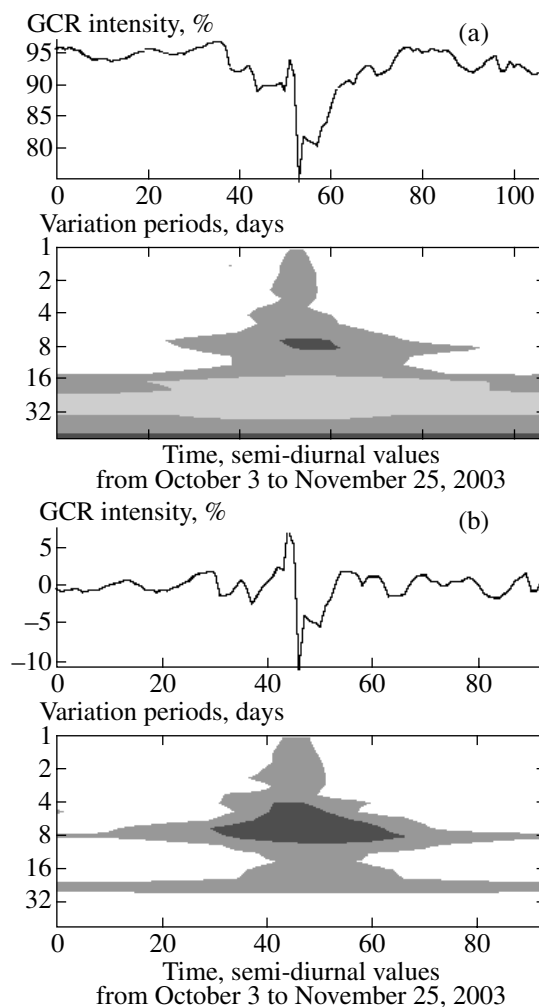


Fig. 1. Results of a wavelet analysis of the GCR intensity fluctuations (percent) based on (a) the initial data and (b) with eliminated trend. Vertical axis: variation periods (days). Time axis: semidiurnal values of the GCR intensity.

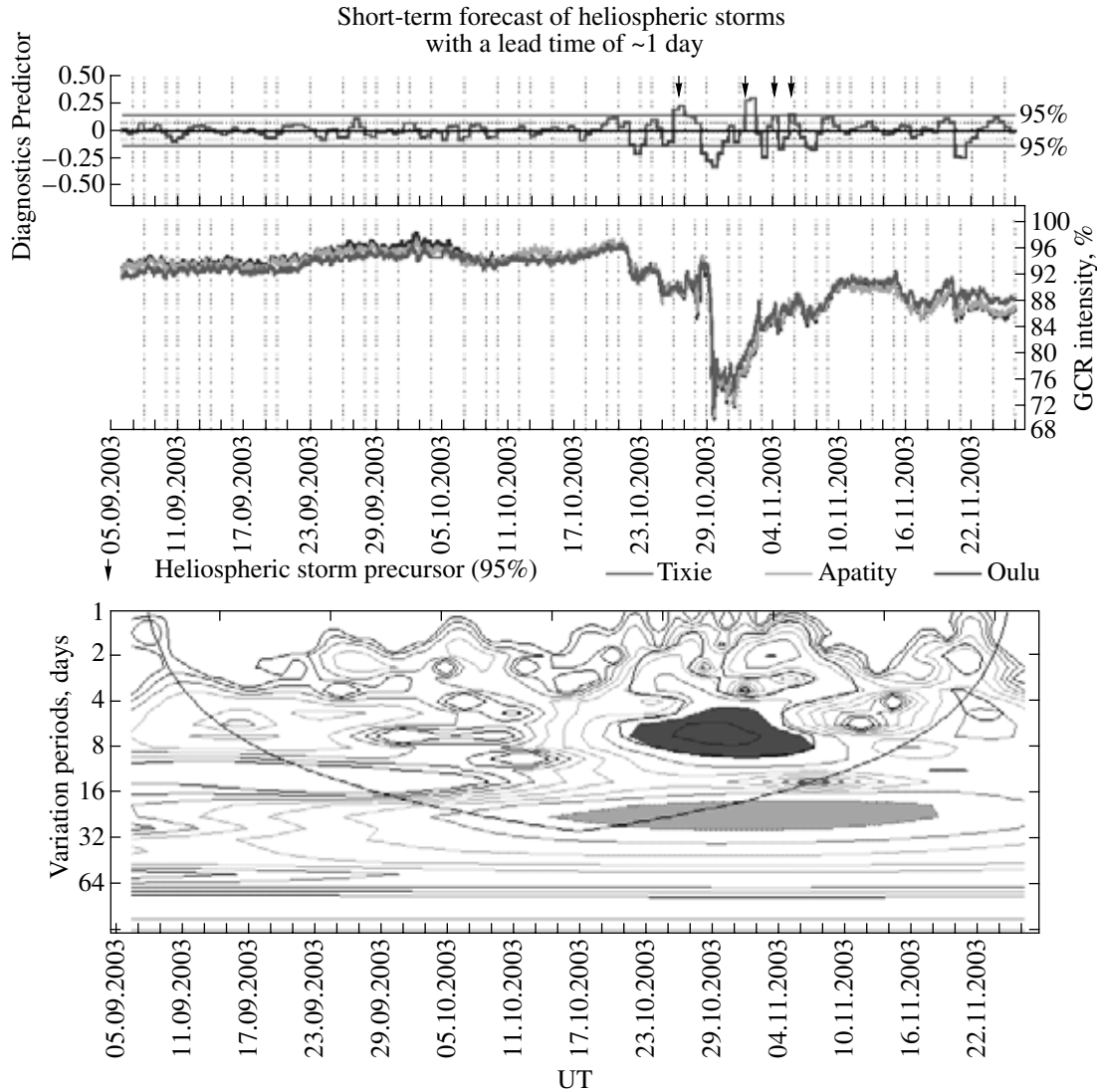


Fig. 2. Results of cosmic ray monitoring and a wavelet analysis of variations in the GCR scintillation index in October–November 2003. Two horizontal lines: bilateral 95% significance level for the scintillation index. Significant positive values correspond to the predictor; negative values, to diagnostics. Bottom, vertical axis: variation periods (days). Horizontal axis: diurnal UT scale.

a wavelet analysis of the GCR fluctuations for the data without the trend are shown at the bottom of Fig. 1. The spectral–temporal analysis of GCR intensity fluctuations using a wavelet analysis allows us to reveal the characteristic dynamics of GCR intensity fluctuations, found for the first time by Kozlov et al. [1973], in the vicinity of the interplanetary shock front. After the elimination of the trend, this dynamics becomes most distinct.

We introduced the spectral–temporal index of GCR scintillations [Kozlov et al., 1984] in order to formalize the detected dynamics. As a result of this formalization, we reduced the dimensionality of the three-dimensional dynamic spectrum of the process to a customary (two-dimensional) numerical sequence of the scintillation

index. This allows us to apply all known methods of quantitative analysis of fluctuations, including a wavelet analysis, to the scintillation index.

3. RESULTS OF ANALYSIS

The results of applying a wavelet analysis to the GCR scintillation index for three solar rotations from September to November 2003 are presented in Fig. 2. We used 5-min data from three polar stations: Tixie Bay, Apatity, and Oulu (Finland). The calculated 5-min values of the GCR scintillation index were averaged over 12 h. Two horizontal lines indicate a bilateral 95% significance level. The positive and significant values of the scintillation index that exceed the 95% level corre-

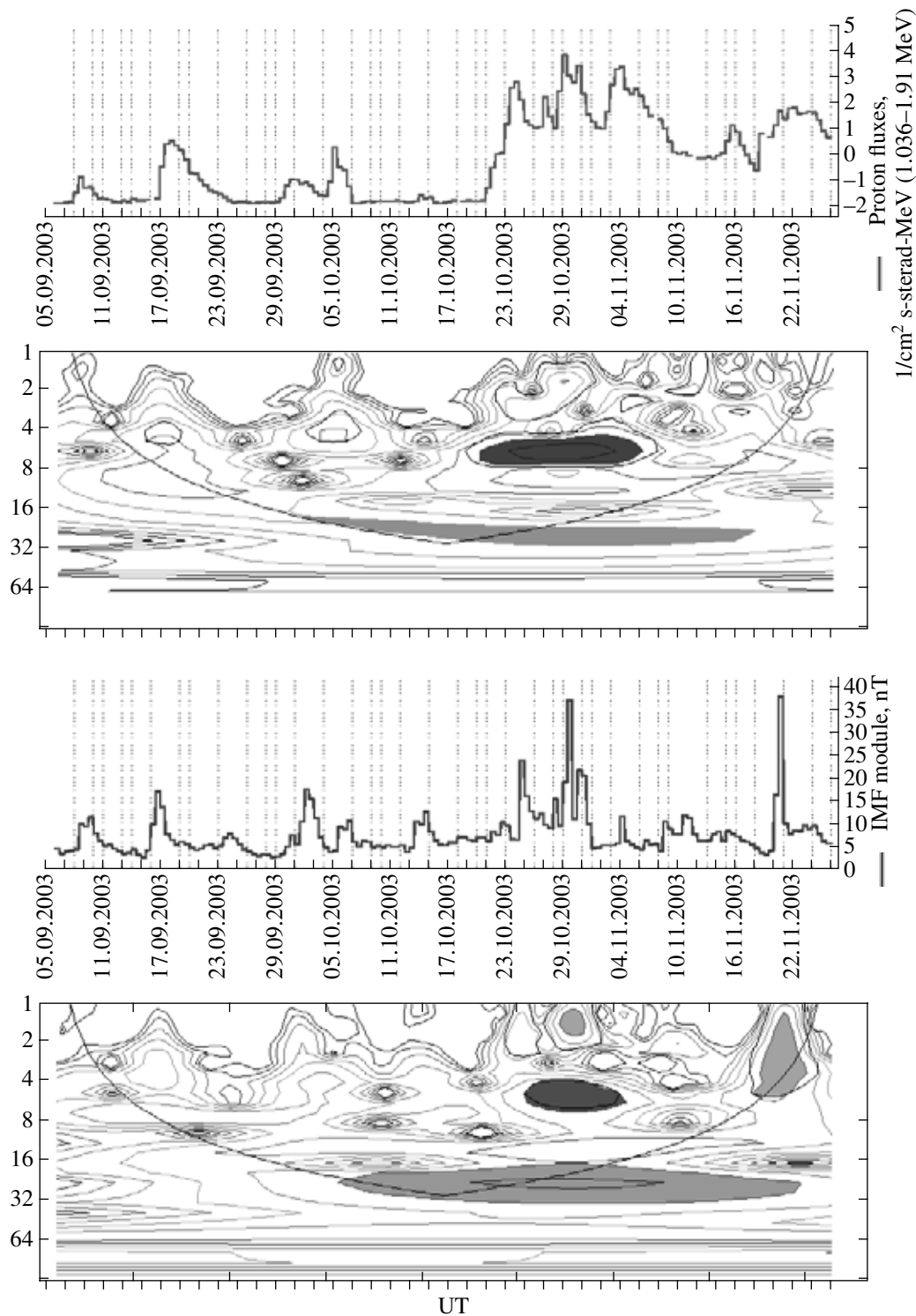


Fig. 3. Time variations and results of a wavelet analysis of the interplanetary medium parameters: flux of low-energy protons and IMF intensity in September–November 2003. Horizontal axis: diurnal UT scale.

spond to the registration of a precursor or predictor. Negative values of the index below the lower layer of significance mean event diagnostics.

The intervals with diagnostic values of the scintillation index exactly correspond to disturbances in the Earth's orbit. First of all, this follows from the time

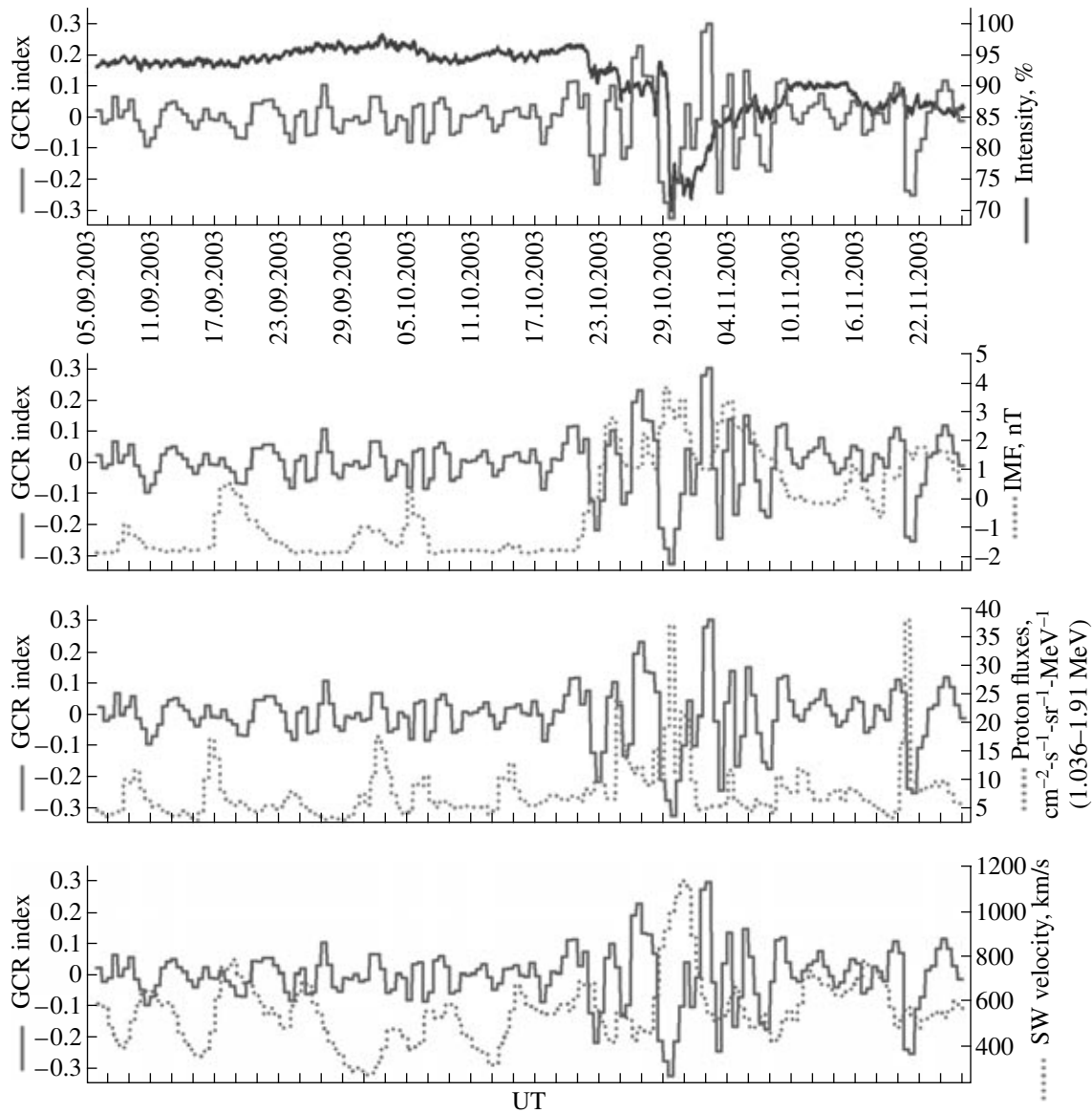


Fig. 4. Comparison of variations in the daily average GCR scintillation index and interplanetary medium parameters: flux of low-energy protons and IMF intensity in September–November 2003. Horizontal axis: diurnal UT scale.

variations in the GCR intensity. The greatest amplitude of variations in the scintillation index is reached in the disturbed period in October–November 2003. Vertical arrows denote the instants of the maximum GCR scintillation index values at the 95% significance level: October 26–27, November 1, 3, and 5. These values are determined as predictors or precursors of the heliospheric storm of October 28–29. The values of the scintillation index for October 20–21 and 24 are at a lower (80%) significance level. The Forbush effects were recorded on October 22 and 25, 2003, respectively.

Before the most powerful event of October 28–29, the longest (since October 26–27) predictor is also recorded. Significant variations in the index were also

recorded at the beginning of November 2003. The weak geoeffectiveness of the powerful November events is related to the displacement of the active region to the western edge of the limb. As a whole, the wavelet image of the variations in the GCR scintillation index in Fig. 2 is similar to the wavelet image of the variations in the GCR intensity (see Fig. 1). In the disturbed period, a non-stationary almost weekly variation is clearly defined. The LF maximum, corresponding to the period of the recurrent 27-day variation, is also present in the spectrum.

Figure 3 presents the results of a wavelet analysis of the interplanetary medium parameters in the studied interval: the flux of low-energy (~1 MeV) protons (on

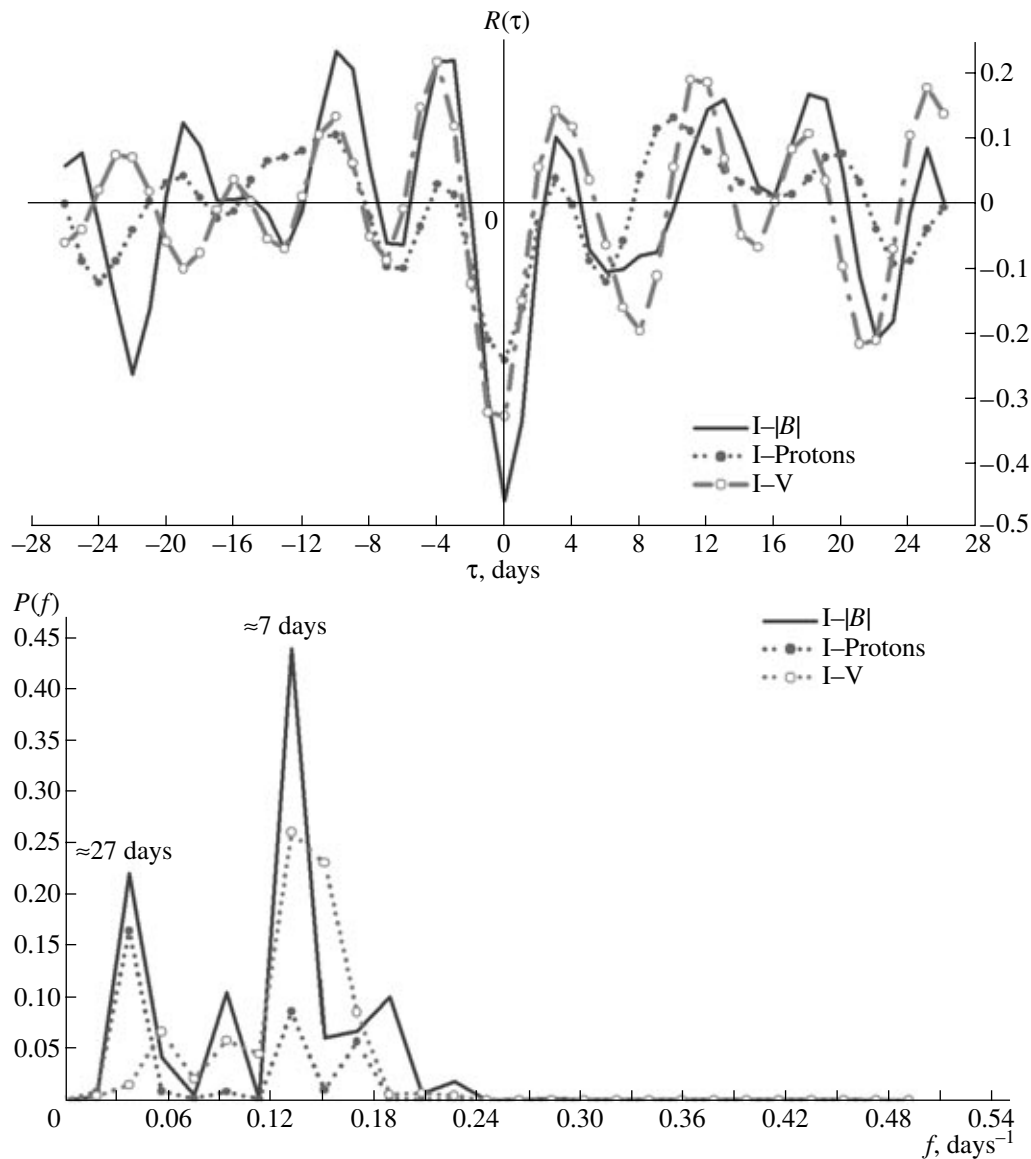


Fig. 5. Results of calculating the cross-correlation functions and their mutual spectra: scintillation index–IMF intensity, scintillation index–proton flux, scintillation index–solar wind velocity. Horizontal axis: shift τ .

the logarithmic scale) and the IMF intensity. The amplitude of variations in the parameters of the medium becomes the largest during a heliospheric storm in cosmic rays. Attention is drawn to the similarity in the dynamics of the structure of variations in the analyzed parameters and in the GCR scintillation index: a non-stationary almost weekly variation appears in the disturbed period against a background of the dominating recurrent 27-day variation. During the heliospheric storm, the maximum of the scintillation index always precedes the maxima in the parameters of the medium (Fig. 4). On the contrary, significant negative (minimum) values of the GCR scintillation index systematically coincide with the maximum values of the analyzed parameters. Precisely this is confirmed by the anticorrelation between the scintillation index and

parameters of the interplanetary medium (Fig. 5). It is important to stress that two harmonics dominate in the mutual spectra: a recurrent variation with a period of ≈ 27 days and an almost weekly variation with a period of ≈ 7 days.

Figure 6 shows the results of the cosmic ray monitoring during the events in July 2004 based on the data of three high-latitude neutron monitors (Tixie Bay, Apatity, and Oulu). As in October–November 2003, the greatest amplitude of significant variations in the GCR scintillation index is observed in the disturbed period.

During three solar rotations, predictors were recorded at the 95% significance level only thrice: on July 21/22, 25/26, and 29/30. Decreases in the GCR intensity were observed on July 22–23, July 27, and

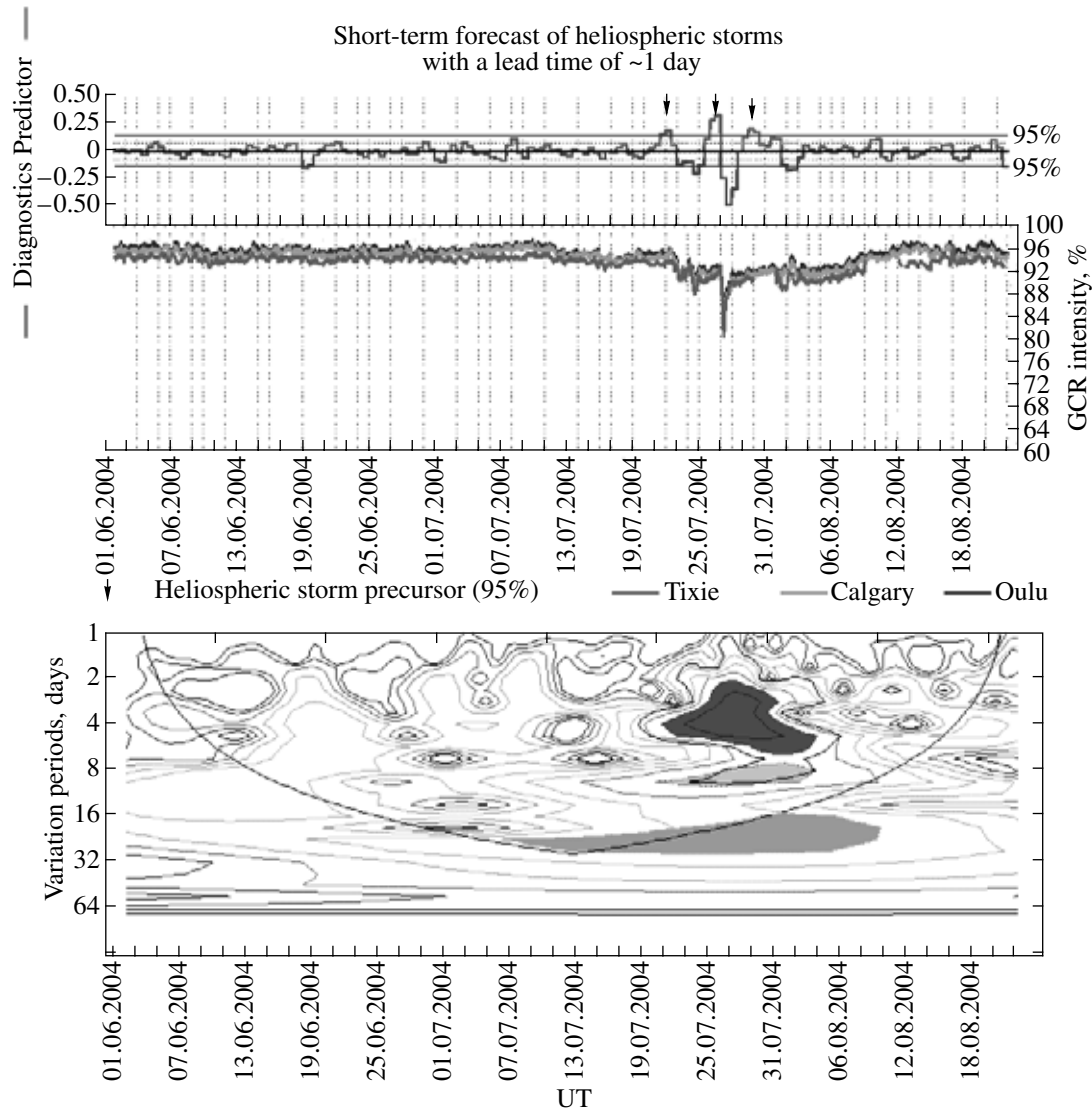


Fig. 6. The same as in Fig. 2 but for the interval from June 1 to August 21, 2004.

August 1, respectively. At the bottom of Fig. 6, a wavelet analysis of the variations in the scintillation index in the analyzed period is presented. On the whole, the wavelet image of the large-scale disturbance in July 2004 is similar to the wavelet image of the event in October–November 2003, with the exception that the period of the activity wave is $T = 4 \pm 1$ days in this case. As in the previous event in October 2003, the same recurrent variation with the 27-day period was observed in July 2004. The second harmonic of the recurrent variation with a period of 13–14 days is also noticeable.

Not less powerful events were observed in the summer and autumn of 2005. The powerful July event with a complex two-stage structure was preceded by a record of two storm predictors on July 8 and 15–16 (Fig. 7). The GCR intensity decreased on July 9–10 and 17–18,

respectively. Before an isolated Forbush effect (6–7%) on August 24, the index of GCR scintillations was recorded only at an 80% significance level. This isolated decrease in the GCR intensity was caused by an active region emerging in the visible (western) part of the solar disk, which appeared again in the visible part of the disk on September 7, 2005.

On September 8 at 0315 UT, the Arctic Prognosis Center of the Institute of Cosmophysical Research and Aeronomy recorded a predictor with a subsequent Forbush effect on September 9–11 (Fig. 8) with an amplitude of $\approx 10\%$ (cosmoprognoz@ikfia.ysn.ru). In this case we have in the pure form (no other active regions on the solar disk) the so-called effect of an “ascend” of an active region onto the visible part of the solar disk. The effect of “ascend” was detected for the first time during the real-time monitoring of GCR scintillations

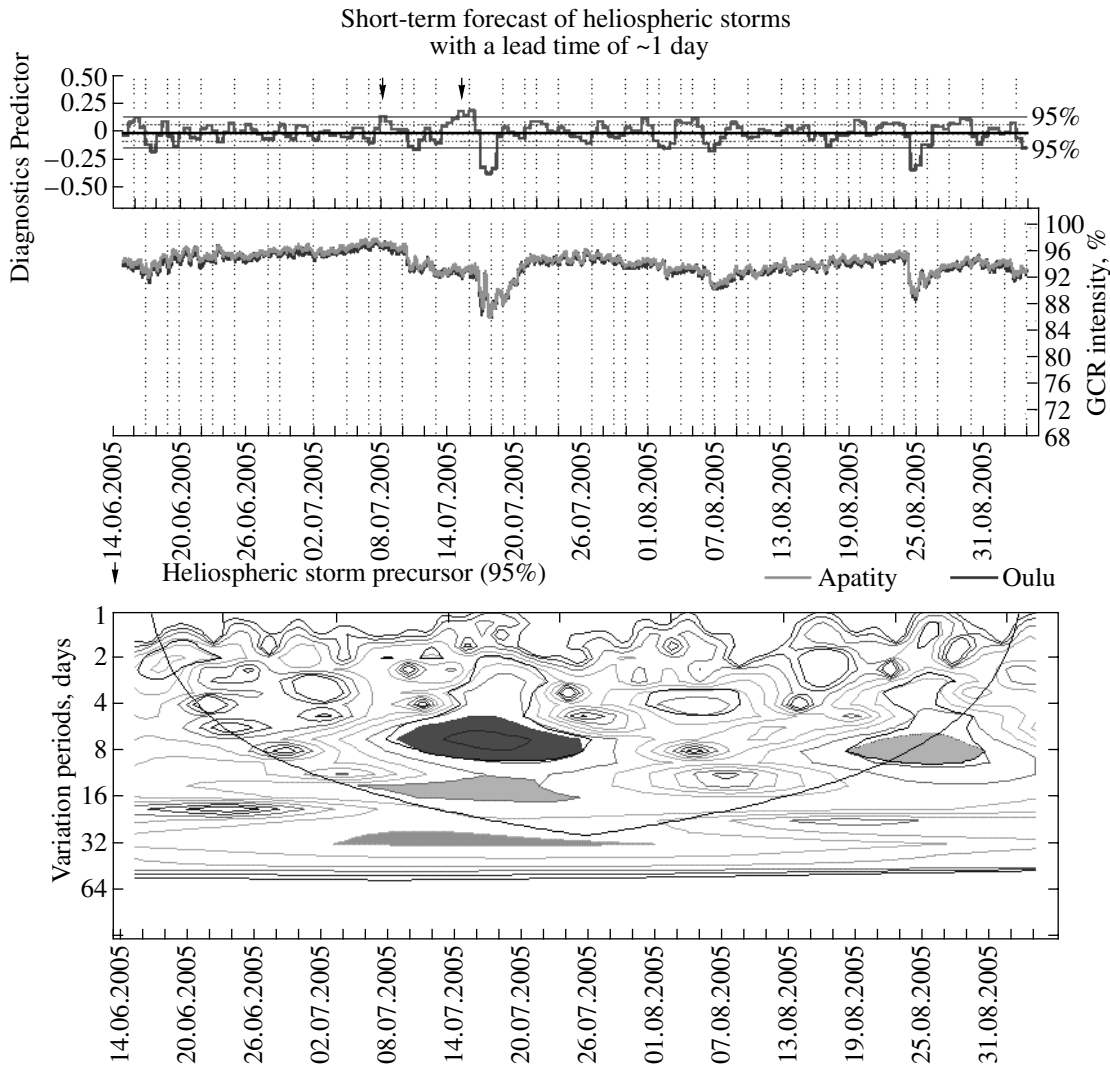


Fig. 7. The same as in Fig. 2 but for the interval from June 14 to September 3, 2005.

at Tixie Bay Polar Geocosmophysical Observatory in July 1982 [Kozlov et al., 1984] and was subsequently confirmed during an analysis of several events in 1984 and 1985 [Kozlov and Krymsky, 1993].

4. DISCUSSION OF RESULTS

Various events in the active interval of 2003–2005 have, nevertheless, many common features in the wavelet representation. We can finally speak about a characteristic scenario of the dynamics of variations in the GCR scintillation index. This scenario consists in a sequential record, first, of a recurrent variation with a period of 27 days, then, of its second harmonic with a period of 14 ± 1 days and, further, of an oscillation with an almost weekly period $T = 5 \pm 2$ days, or of an “activity wave” [Tugolukov and Kozlov, 1991; Kozlov and Tugolukov, 1992]. Below the same events of 1991 are

analyzed by the modern method of a wavelet analysis (Fig. 9).

From January to February 1991, no storm predictors were observed. A significant precursor was recorded only on March 23 before a sharp and deep Forbush effect of March 24. The recurrent 27-day variation, which dominated at the beginning, was transformed during the disturbed period into the 13–14-day variation and, further, into an almost weekly activity wave.

The above scenario of the dynamics of the HCS structure is fairly consistent with the dynamics of the HCS structure caused by variations in the ratio of the quadrupole component of the solar magnetic field to its dipole part during the sign reversal of the global solar magnetic field. Indeed, it is known that variations in the ratio the quadrupole-to-dipole components manifest themselves in the HCS structure: two-sector in the case

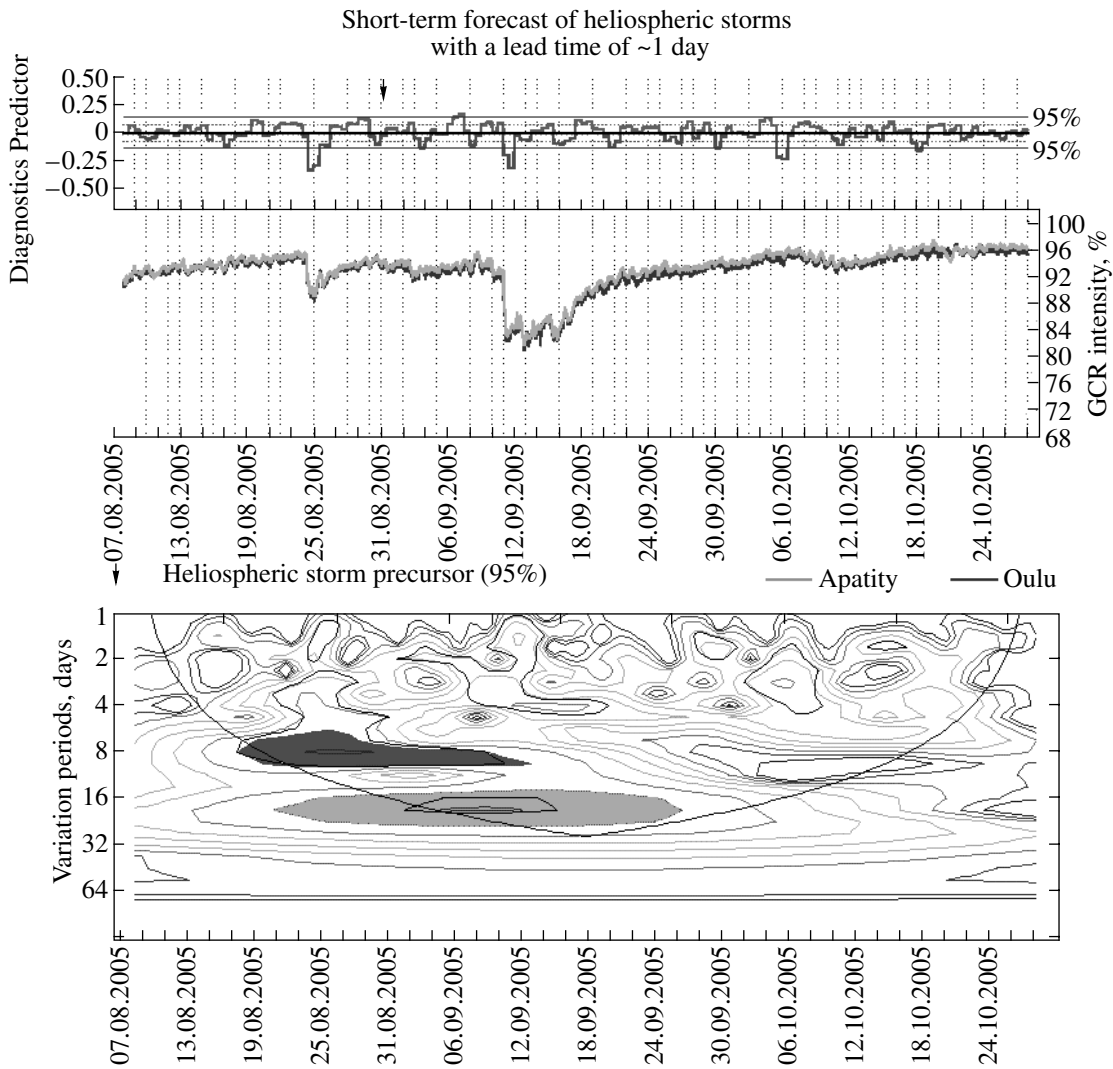


Fig. 8. The same as in Fig. 2 but for the interval from August 7 to October 27, 2005.

of dipole (27-day variation) and four-sector for quadrupole components [Sunderson et al., 2003].

It seems that the revealed scenario of the dynamics of the HCS structure is directly related to the problem of origin of the most powerful Forbush effects with a composite structure (two-stage, etc.) of a heliospheric storm in cosmic rays. The absence of the generally accepted definition of a Forbush effect indicates that the origin of this effect is insufficiently clear. This was earlier referred to by a number of researchers [Sanderson et al., 1990; Bavassano et al., 1991; Nagashima et al., 1992; Kozlov, 1995], including one of the recent works on this subject [Belov et al., 2001]. The latest publications, in which the complexity of the problem of identification of disturbing sources recorded in the Earth’s orbit was noted [Manoharan et al., 2004; Zhang et al., 2004], are not an exception.

Earlier Kozlov [1980] defined the Forbush effect as a “result of modulation of cosmic rays gas by a packet of interacting hydromagnetic waves of different scales”. By virtue of self-similar or fractal properties peculiar to the structure of the GCR intensity decreases of different scales [Kozlov, 1999], a similar definition can also be accepted for a heliospheric storm in cosmic rays, with the exception that the word combination emphasized above should be replaced by the following in both cases: by a *soliton-like packet (soliton of the envelope) of hydromagnetic waves*. This is confirmed by the wavelet image (found using the modern methods of analysis) of the heliospheric storm in cosmic rays (and not only) and by the results of a joint analysis of the GCR scintillation index and parameters of the interplanetary medium in the studied interval.

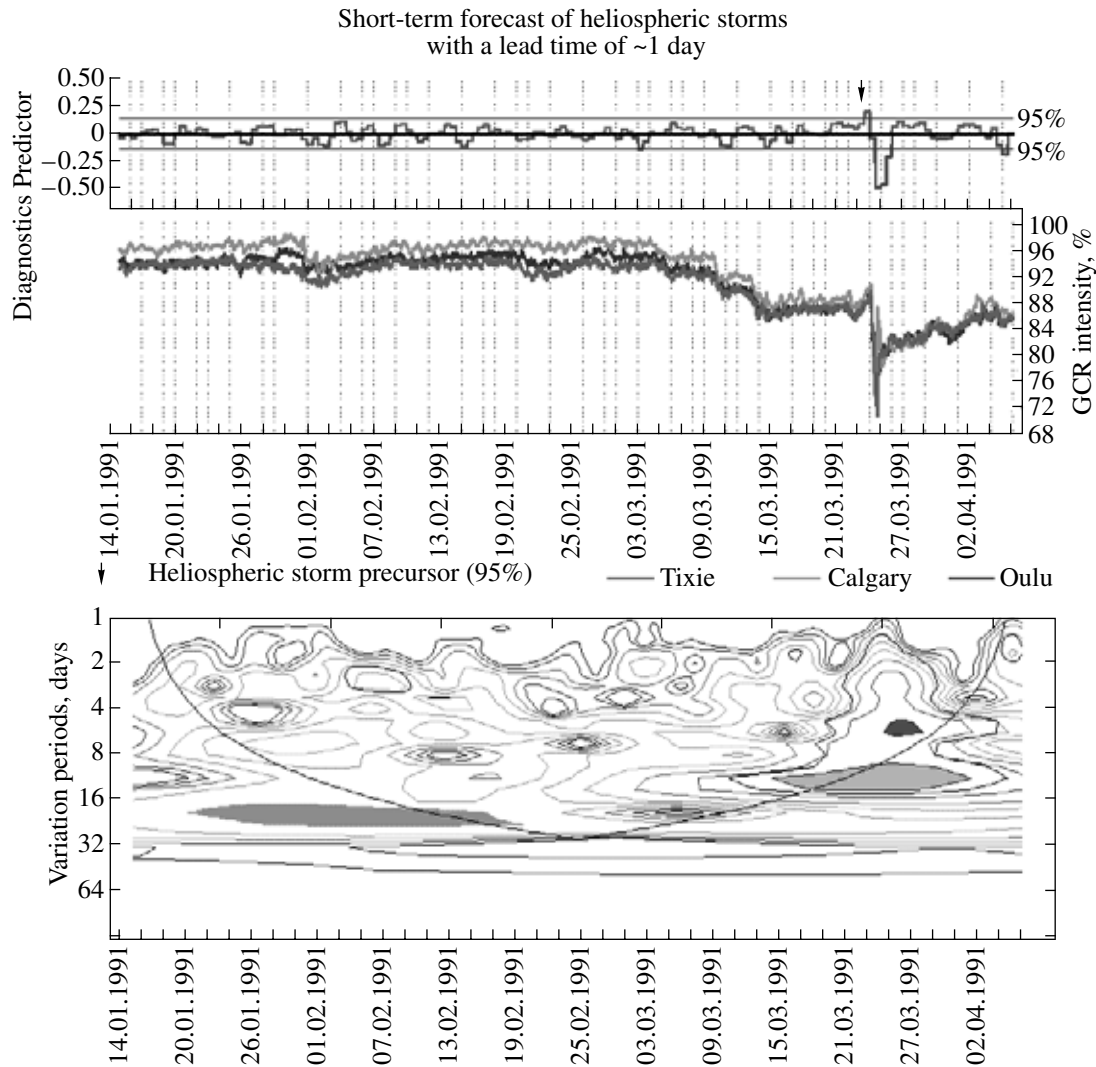


Fig. 9. The same as in Fig. 2 but for the interval from January 14 to April 5, 1991.

5. CONCLUSIONS

During the sign reversal of the global solar magnetic field, the variations in the ratio of the quadrupole component of the field to its dipole part manifest themselves in a change of the structure of the heliospheric current sheet from the two-sector to four-sector and, then, to multisector structure. At that time, a soliton-like wave packet (soliton of the envelope) is formed in HCS, precisely which is responsible for the wavelet image of the heliospheric storm in cosmic rays.

ACKNOWLEDGMENTS

We are grateful to the University of Oulu, Sodankylä Geophysical Observatory (Finland, <http://cosmicrays oulu.fi/>), and Polar Geophysical Institute (Apatity, <http://pgi.kolasc.net.ru/>) for presented 5-min neutron monitor data.

This work was supported by the Leading Science School, Russian Academy of Sciences, grant NSh-422.2003.2 (Academician G.F. Krymsky).

REFERENCES

1. B. Bavassano, A. Felici, and M. Storini, "Travelling Interplanetary Perturbations and Related Phenomena," in *Proceedings of the First SOLTIP Symposium, Liblice, 1991*, Vol. 2, pp. 14–19.
2. A. V. Belov, E. A. Eroshenko, V. A. Oleneva, et al., "What are the Causes of Forbush Effects?" *Izv. Akad. Nauk, Ser. Fiz.* **65** (3), 373–376 (2001).
3. V. I. Kozlov and N. N. Tugolukov, "CR Intensity Scintillations," *Geomagn. Aeron.* **32** (3), 153–159 (1992).
4. V. I. Kozlov and P. F. Krymsky, *Physical Backgrounds of Predicting Catastrophic Geophysical Phenomena* (YaNTs SO RAN, Yakutsk, 1993).

5. V. I. Kozlov, "On the Relation between Forbush Decreases and Passages of the Sector Boundaries of the Heliospheric Current Sheet," *Izv. Akad. Nauk, Ser. Fiz.* **59** (4) (1995).
6. V. I. Kozlov, "Estimation of the Scaling Features of Cosmic Ray Fluctuation Dynamics in the Solar Cycle," *Geomagn. Aeron.* **39** (1), 100–104 (1999) [*Geomagn. Aeron.* **39**, 95–98 (1999)].
7. V. I. Kozlov, "CR Pulsation Origin," *Geomagn. Aeron.* **20** (3), 391–395 (1980).
8. V. I. Kozlov, A. I. Kuzmin, G. F. Krymsky, et al., "Cosmic Ray Variations with Periods Less than 12 Hours," in *Proceedings of the 13th ICRC, Denver, 1973*, Vol. 2, pp. 939–942.
9. V. I. Kozlov, D. Z. Borisov, and N. N. Tugolukov, "Method for Diagnosing Interplanetary Disturbances Based on Studying CR Fluctuations and Method Realization in the System of Automation of the Research at Tixie Bay Observatory," *Izv. Akad. Nauk SSSR, Ser. Fiz.* **48** (11), 2228–2230 (1984).
10. P. K. Manoharan, N. Gopalswamy, S. Yashiro, et al., "Influence of Coronal Mass Ejection Interaction on Propagation of Interplanetary Shock," *J. Geophys. Res.* **109A**, (2004).
11. K. Nagashima, K. Fujimoto, S. Sakakibara, et al., "Local-Time-Dependent Pre-IMF-Shock Decrease and Post-Shock Increase of Cosmic Rays, Produced Respectively by Their IMF-Collimated Outward and Inward Flows across the Shock Responsible for Forbush Decrease," *Planet. Space Sci.* **40** (8), 1109–1137 (1992).
12. T. R. Sanderson, J. Beeck, R. G. Marsden, et al., "Cosmic Ray, Energetic Ion and Magnetic Field Characteristics of a Magnetic Cloud," in *Proceedings of the 21st ICRC, Adelaide, 1990*, Vol. 6, pp. 251–258.
13. T. R. Sanderson, T. Appourchaux, J. T. Hoeksema, and K. L. Harvey, "Observations of the Sun's Magnetic Field during the Recent Solar Maximum," *J. Geophys. Res.* **108A**, 1035 (2003).
14. N. N. Tugolukov and V. I. Kozlov, "Relation between CR Intensity Scintillations and Solar Wind Parameters," *Geomagn. Aeron.* **31** (4), 715–716 (1991).
15. Zhang Jichun, Michael W. Liemohn, Janet U. Kozyra, et al., "A Statistical Study of the Geoeffectiveness of Magnetic Clouds during High Solar Activity Years," *J. Geophys. Res.* **109A**, (2004).